

# Time evolution of probability density function of gamma ray burst (GRB) - a possible indication of turbulence origin of GRB

Nilay Bhatt<sup>1\*</sup> Subir Bhattacharyya<sup>1 †</sup>

<sup>1</sup>*Astrophysical Sciences Division, Bhabha Atomic Research Centre, Mumbai 400085, India*

14 November 2011

## ABSTRACT

Gamma ray burst (GRB) time series is a non-stationary time series with all its statistical properties varying with time. Considering that each GRB is a different manifestation of the same stochastic process we studied the time dependent as well as time averaged probability density function (*pdf*) characterizing the underlying stochastic process. The *pdfs* are fitted with Gaussian distribution function and it has been argued that the Gaussian *pdfs* possibly indicate the turbulence origin of GRB. The spectral and temporal evolution of GRBs are also studied through the evolution of spectral forms, color-color diagrams and hysteresis loops. The results do not contradict the turbulence interpretation of GRB.

**Key words:** Gamma-ray burst – X-rays – cross-correlation – time lag.

## 1 INTRODUCTION

Even after the three decades of extensive observations of gamma-ray burst (GRB) prompt emission there is no conclusive idea about the energy dissipation mechanism and the radiative process responsible for high energy emission (Lyutikov (2009); Ghisellini (2010)). In the *standard model* of GRB, known as fireball model (Goodman (1986); Paczynski (1986); Shemi & Piran (1990); Meszaros & Rees (1993); Rees & Meszaros (1992); Sari & Piran (1995); Kobayashi et al. (1999); Mészáros & Rees (2000); Mészáros et al. (2002)), the bulk energy associated with the relativistic expansion of the fireball, is dissipated into the random energy of particles through internal shocks. Internal shocks are produced due to the time dependent speed of the relativistic outflow (Kobayashi et al. (1997); Rees & Meszaros (1994); Sari & Piran (1997)). But it is now established that the internal shock model suffers from different shortcomings, particularly, the low radiation efficiency, problem of baryon loading and the large dissipation radius (Narayan & Kumar (2009); Lazzati & Begelman (2010)).

As possible alternatives of internal shock model, Lyutikov & Blandford (2003) and Lyutikov (2006) proposed electromagnetic model of gamma-ray burst whereas Narayan & Kumar (2009) discussed relativistic turbulence

model for GRB. In electromagnetic model the GRB outflow is considered as Poynting flux dominated wind (Lyutikov (2006)). The energy dissipation and particle acceleration occur through magnetic dissipation process, mainly through magnetic reconnection. In relativistic turbulence model by Narayan & Kumar (2009), it is considered that the fluid in GRB outflow is relativistically turbulent. The rapid variability in the GRB lightcurve arise due to the relativistic random velocity fluctuations of radiation emitting eddies formed in the turbulence. The model was successfully applied to explain the X-ray–gamma-ray and optical emission during the prompt phase of the brightest *Swift* gamma-ray burst GRB080319B (Kumar & Narayan (2009)).

A photospheric emission model is proposed by Lazzati & Begelman (2010) very recently. Generally the photosphere, associated with the fireball, is dominated by thermal radiation. It is assumed that the electrons, energised by some shock or due to magnetic reconnection, Comptonize the thermal photons in an optically thick medium. The multiple Comptonization leads to a power-law photon distribution in the keV–MeV region whereas a thermal peak remains in the keV energy range. The main advantage of this model is that it does not require any efficient dissipation mechanism and the radiative efficiency of this model is also very high. But there is no strong observational evidence of any thermal component in GRB spectra.

As far as the spectral studies are concerned, the majority of observed time averaged prompt emission spectra of GRBs

\* E-mail: nilayb@barc.gov.in

† E-mail: subirb@barc.gov.in

are fitted with Band function (Band et al. (1993)) which, indeed, is no more than a mathematical function having no physical interpretation yet. It is generally believed that the high energy emission in the prompt phase is due to the synchrotron process (Tavani (1996a,b)). But the detail study of BATSE GRBs shows that for many GRBs the low energy spectral slopes are not consistent with the theory of synchrotron emission (Preece et al. (2000)).

Therefore to have deeper understanding on the physical processes occurring in gamma-ray bursts it would be beneficial to study the time evolution of GRB spectra. It is also important to look into the GRB time series from a different perspective and characterise the underlying process. Lloyd-Ronning & Petrosian (2002); Ghirlanda et al. (2002); Medvedev (2006) and several other authors studied the time evolution of GRB spectra for BATSE GRBs. Lloyd-Ronning & Petrosian (2002) studied a 128 ms spectra for a large sample of GRBs observed by BATSE. The spectra were fitted with synchrotron emission model where the spectra were calculated in three emission regime, such as, for isotropic pitch angle emission of electrons, for small angle pitch angle distribution of electrons and for self-absorbed systems. Eventhough the spectral fitting were done and the time evolution of spectral index and normalization were studied, but the physical description was not self-consistently developed within the framework of fireball model. Ghirlanda et al. (2002) also studied BATSE GRBs and fitted the time resolved spectra with Band function, broken power-law, thermal Comptonization and synchrotron shock model. It was concluded that the behaviour of the time resolved spectra is not consistent with the time integrated spectrum. The low energy spectral indices also violates the synchrotron spectral limit.

In this paper we studied the probability density function (*pdf*) and spectral evolution of four bright GRBs detected by *Swift* and tried to find out if there is any systematics among those GRBs. In Beloborodov et al. (2000), the authors mentioned that the individual burst is a random realization of the same standard stochastic process. In any stochastic process there is an underlying *pdf* which characterises the process. Therefore it is important to find out the *pdf* from GRB time series to identify if it has any general characteristic. Since GRBs are highly non-stationary process, we calculated time-dependent as well as time averaged *pdf* for selected GRBs. We also studied the spectral evolution, colour-colour and hardness-count rate correlations for those GRBs.

In Section 2 we give a brief description of the selected GRBs, in Section 3 we describe the analysis procedure of *Swift*-BAT data. Results are described and discussed in Sections 4 and we conclude the paper in Section 5.

## 2 SELECTED GRBS

We have analysed the *Swift*-BAT data for GRB050525, GRB061121, GRB080319b and GRB080411. GRBs are selected based on their fluence. All four GRBs have fluence  $> 10^{-5}$  erg cm $^{-2}$ . For the sake of completeness we give a brief description each GRB below.

- **GRB050525** : This GRB was observed with *Swift*-BAT in the energy range 15–350 keV. It is at a redshift of

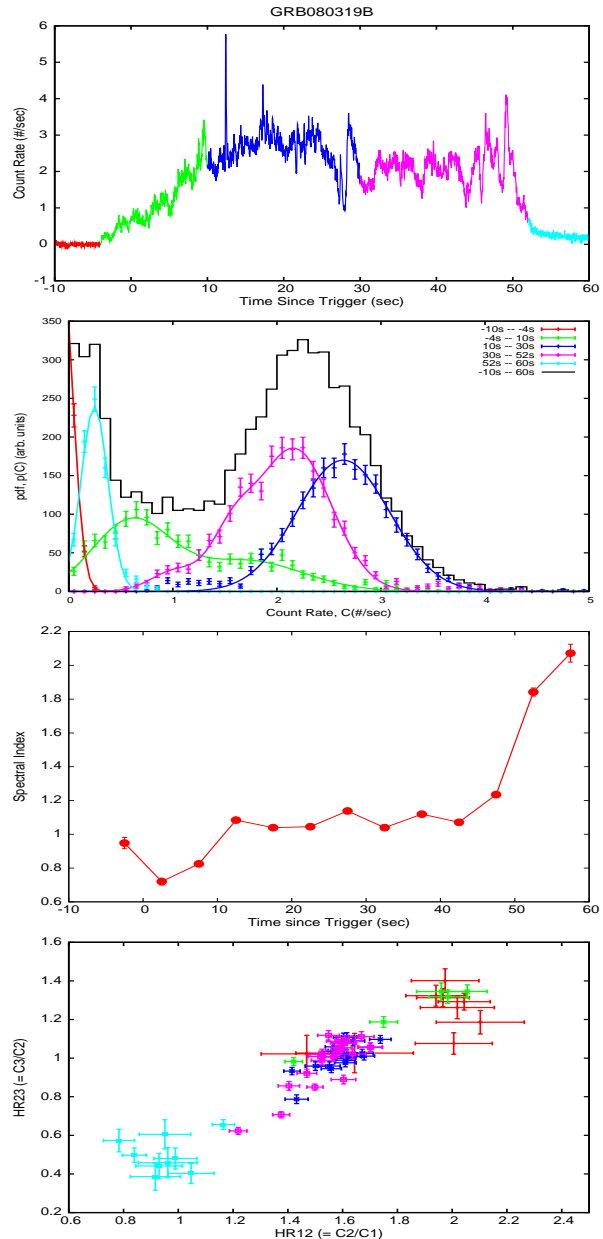


**Figure 1.** *First panel* (from top) : Lightcurve of GRB080319b; *second panel* : probability density function - time averaged (black), time dependent (colours of different distributions correspond to the portions of the lightcurve with same colour); *third panel* : variation of spectral index with time; *fourth panel* : colour-colour diagram for the active portion of the lightcurve (same colour convention maintained).

0.606. The observed fluence in the *Swift*-BAT energy range is  $1.86 \times 10^{-5}$  ergs cm $^2$ . The time averaged spectrum in the 15–350 keV range was fitted with a power-law ( $\sim \nu^{-\alpha}$ ) with spectral index 0.83. The estimated isotropic energy is  $E_{iso} = 1.94 \times 10^{52}$  erg (Band et al. (2005); Markwardt et al. (2005)).

- **GRB061121** : *Swift*-BAT detected this burst along with a precursor. Here we concentrate on the main event which has  $T_{90} = 18.2 \pm 1.1$  s. The *Swift*/BAT spectrum was fitted with a power-law with spectral index 1.375. The

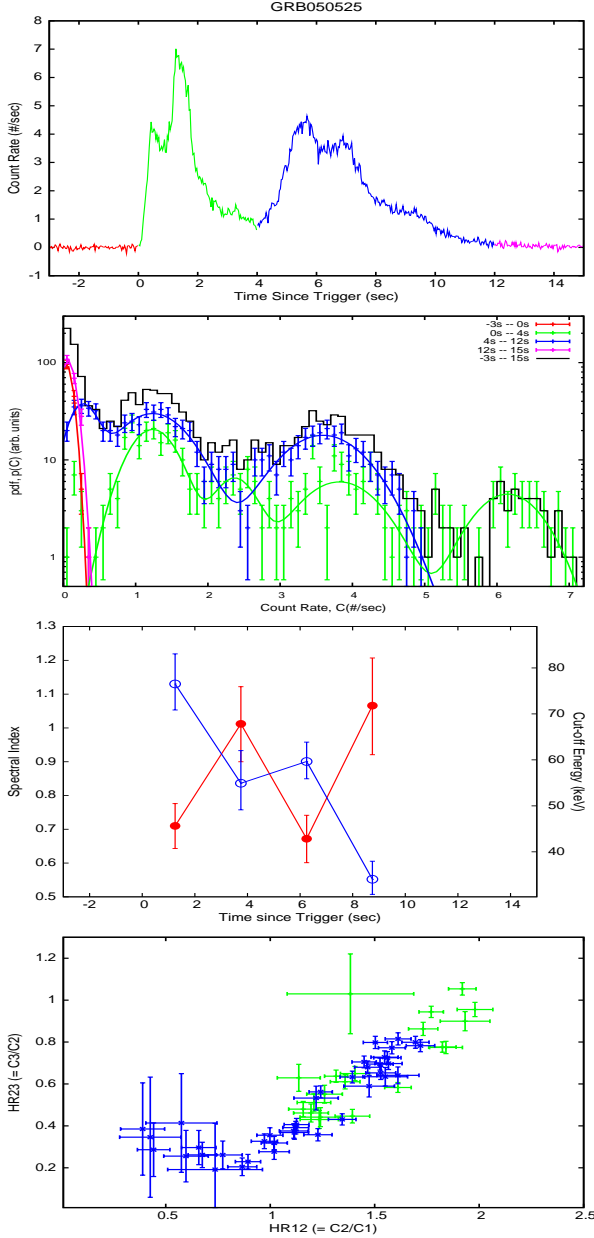


Figure 2. Same as Figure 1, but for GRB050525.

measured fluence is  $2.792 \times 10^{-5}$  erg cm $^{-2}$ . The measured redshift for the burst is 1.314 which leads to a measured isotropic energy  $E_{iso} \approx 6.7 \times 10^{53}$  erg. Page et al. (2007) studied the broadband spectral evolution of the prompt and afterglow emission of the burst.

- **GRB080411** : GRB080411 consists of two strong peaks which are widely separated in time. The time averaged spectrum in the *Swift*/BAT energy range was fitted with a power-law with spectral index 1.678. The observed fluence is  $4.3 \times 10^{-5}$  erg cm $^{-2}$ . The measured redshift of the burst is 1.03 which gives an isotropic energy of the burst  $\sim 4.04^{53}$  erg (Marshall et al (2008)).

- **GRB080319b** : This gamma-ray burst is one of the brightest GRBs with a very strong optical flash during its prompt emission. This GRB was simultaneously observed with *Swift*-BAT and *Konus-Wind* in the energy range 15–

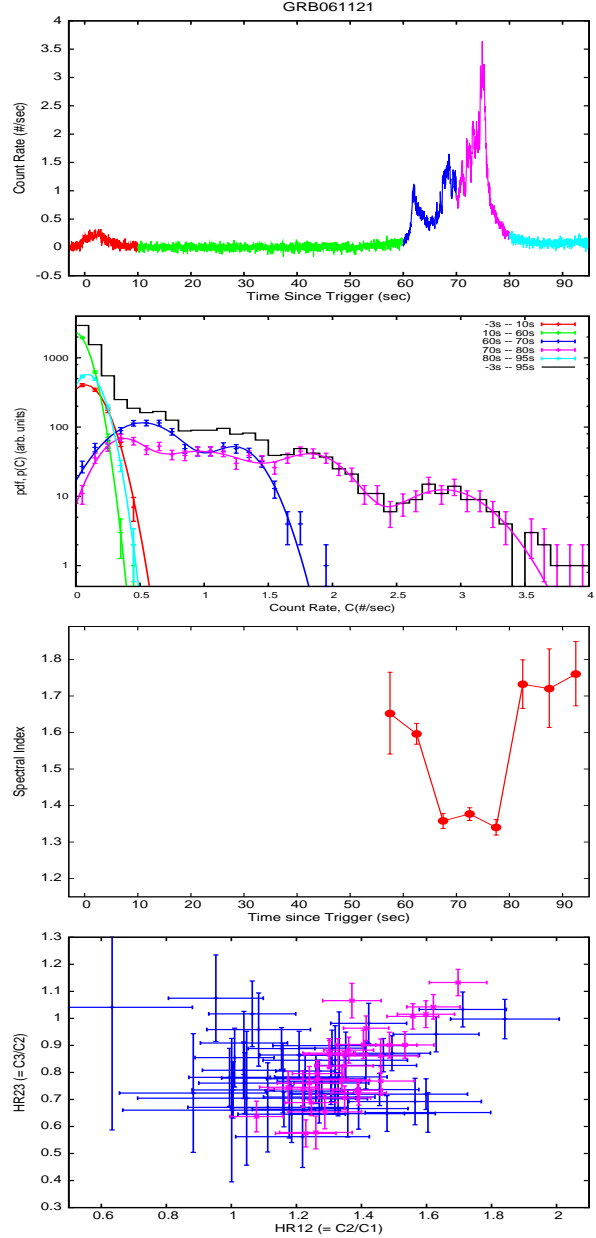
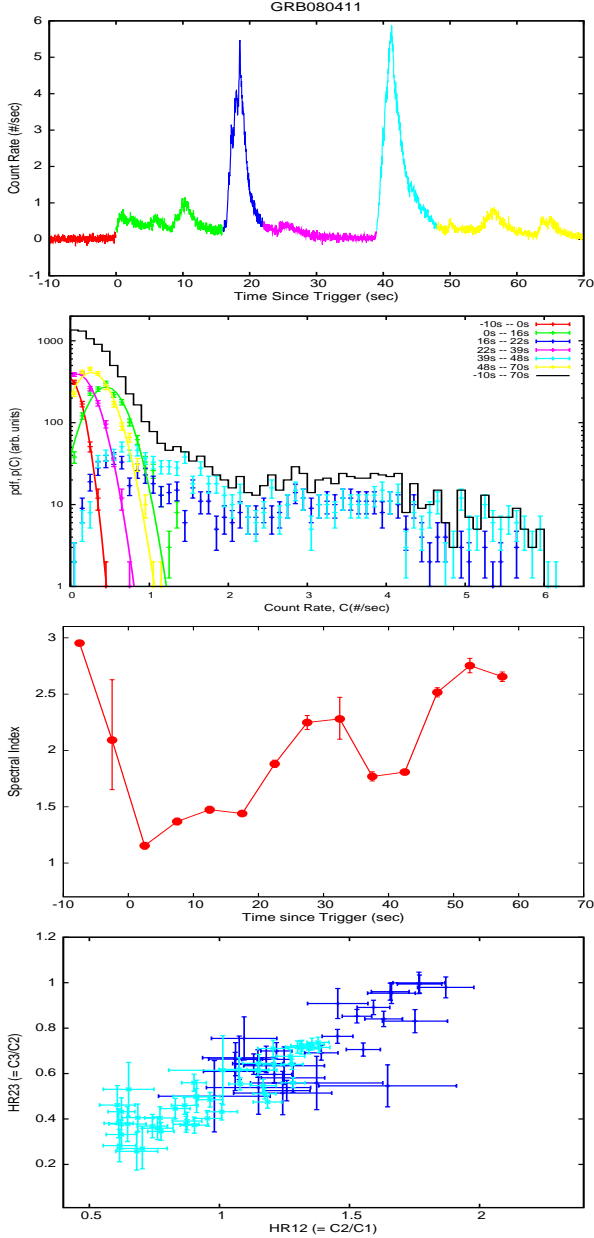


Figure 3. Same as Figure 1, but for GRB061121.

350 keV and 18–1160 keV respectively. The observed fluence in the 20keV–7MeV band is  $5.7 \pm 10^{-4}$  erg cm $^{-2}$ . The measured redshift is 0.937 and isotropic energy is estimated to be  $1.3 \times 10^{54}$  erg. The time averaged spectrum measured by *Konus-Wind* was fitted by a broken power-law with break energy at  $E_{br} = 650$  keV. The spectral index below 650 keV is  $0.18 \pm 0.01$  and above 650 keV is  $2.87 \pm 0.44$ . This GRB was also followed by other telescopes in different wavelengths during the prompt and afterglow emission. During the prompt emission it was observed by the *TORTORA* telescope in the optical region and it is discussed in detail by Racusin et al. (2008). This GRB is studied quite extensively by several authors (Zou et al. (2009); Kumar & Narayan (2009)). The most significant feature of this particular GRB is that the time averaged spectrum can not be explained by the synchrotron-self-Compton (SSC)



**Figure 4.** Same as Figure 1, but for GRB080411.

process in the framework of internal shock model. Rather a physically reasonable set of parameters can be obtained in the framework of turbulence model (Kumar & Narayan (2009)).

### 3 DATA ANALYSIS

We analysed *Swift*/BAT event data for four *Swift* detected gamma -ray bursts GRB050525, GRB061121, GRB080411 and GRB080319b. The standard BAT software and the calibration database (CALDB : 20090130) have been used to obtain the lightcurves and the spectra for all four GRBs. We extracted lightcurves with 10 ms time resolution in the energy band 15–150 keV for all GRBs. We also obtained lightcurves in the energy bands  $E_1$  : 15–25 keV,  $E_2$  : 25–50

**Table 1. GRB080319B:** The fitted parameters, their uncertainties and the goodness-of-fit parameter for the Gaussian distribution(s) corresponding to each *pdf*. The colours used to plot the *pdfs* are also given in column 1. For the first time segment, as the *dof* is zero, the fit is a representative one.

Time (sec)	Gaussian Parameters				$\chi^2/\nu$
	$M$	$A_i$	$\mu_i$	$\sigma_i$	
-10 — -4 (red)	1	429.7	-0.07	0.11	—
-4 — 10 (green)	2	$93.8 \pm 4.4$ $39.6 \pm 3.0$	$0.66 \pm 0.03$ $1.89 \pm 0.06$	$0.42 \pm 0.03$ $0.40 \pm 0.04$	23.16/22
10 — 30 (blue)	1	$170.1 \pm 4.6$	$2.64 \pm 0.01$	$0.44 \pm 0.01$	17.13/20
30 — 52 (magenta)	3	$26.5 \pm 8.6$ $59.5 \pm 25.8$ $184.8 \pm 11.6$	$1.02 \pm 0.17$ $1.57 \pm 0.08$ $2.16 \pm 0.05$	$0.23 \pm 0.09$ $0.21 \pm 0.1$ $0.36 \pm 0.03$	27.46/18
52 — 60 (cyan)	2	$235.9 \pm 44.9$ $24.1 \pm 24.0$	$0.23 \pm 0.004$ $0.43 \pm 0.34$	$0.11 \pm 0.01$ $0.21 \pm 0.13$	0.85/3

**Table 2. GRB050525:** Same as Table 1 For the last time segment, as the *dof* is zero, the fit is a representative one.

Time (sec)	Gaussian Parameters				$\chi^2/\nu$
	$M$	$A_i$	$\mu_i$	$\sigma_i$	
-3 — 0 (red)	1	$96.5 \pm 9.5$	$0.043 \pm 0.027$	$0.086 \pm 0.014$	0.7/1
0 — 4 (green)	3	$20.6 \pm 2.2$ $6.3 \pm 1.4$ $5.9 \pm 1.0$	$1.23 \pm 0.03$ $2.37 \pm 0.08$ $3.82 \pm 0.09$	$0.32 \pm 0.03$ $0.28 \pm 0.08$ $0.54 \pm 0.09$	40.8/37
4 — 12 (blue)	3	$34.0 \pm 3.5$ $29.9 \pm 1.8$ $17.9 \pm 1.2$	$0.26 \pm 0.02$ $1.24 \pm 0.04$ $3.59 \pm 0.03$	$0.19 \pm 0.03$ $0.48 \pm 0.04$ $0.57 \pm 0.03$	28.5/41
12 — 15 (magenta)	1	113.9	0.001	0.02	—

keV and  $E_3$  : 50–100 keV with time resolution of 200 msec and 1 sec for all GRBs.

The spectra are extracted for every 5 sec from -10 sec with respect to the trigger time for GRB061121, GRB080411 and GRB080319b. In case of GRB050525 spectra are extracted for every 2.5 sec.

## 4 RESULTS AND DISCUSSION

### 4.1 Probability density function

A stochastic process  $\{x(t)\}$ , also known as time series, is an ensemble of real or complex valued functions. Each stochastic process is characterized by a probability density function (*pdf*) depending on the underlying physical process responsible for the generation of the time series (Bendat & Piersol (2010)). Therefore it is always interesting to develop an understanding of the probability density function for a given time series.

A time series can be stationary or non-stationary depending on whether the statistical properties of the time series,

such as mean, variance, are independent of time or not. The gamma-ray burst time series is a real non-stationary time series with statistical properties of the time series vary with time. Here we calculate the time evolution of the *pdf* and the time averaged *pdf* for all four GRBs of our sample. To study the time evolution of the *pdf* we divide the GRB time series into different time segments and for each segment we calculate the *pdf*. If  $\tau$  be the time length of one segment starting at time  $t$  then the *pdf* is defined by

$$p_{t,t+\tau}(x) = \frac{\Delta N_x}{N} \quad (1)$$

where  $\Delta N_x$  the number of trials that the random variable falls between  $x$  and  $x + \Delta x$ ,  $N$  is the total number of trials. The error in  $p(x)$  at  $x$  is given by  $\sqrt{\Delta N_x}$ . For GRB time series  $x$  represents the count rate. The length of the time segment  $\tau$  at time  $t$  is chosen through visual inspection of the GRB time structure. For the time-averaged *pdf*,  $p(x)$  is computed for the complete lightcurve. It is to be noted that in this work we have not used the normalization for  $p(x)$ . The time-averaged *pdf*, *pdfs* for different time segments for each GRB, alongwith their respective lightcurves, are shown in Figures 1–4 (*first* and *second* panel). The different portions of the lightcurve are shown in different colours and their corresponding probability density functions are also given with the same colour. The time resolution of the lightcurve used for the calculation is 10 ms for all GRBs. From the *pdfs* plotted for different time segment for each GRB it is evident that the *pdfs* corresponding to the rising and the falling part of GRBs peak around zero and those are not affected by the other portions of the GRB. As the GRB evolves, the *pdf* also evolves. In almost all cases, the *pdf* for each time segment is fitted with single or multiple Gaussian distributions given by

$$F(x) = \sum_{i=1}^M A_i \exp \left[ -\frac{1}{2} \left( \frac{x - \mu_i}{\sigma_i} \right)^2 \right] \quad (2)$$

where  $M \geq 1$ . For all GRBs, the parameters of the fitted Gaussian function(s), their uncertainties and the goodness-of-fit parameter are listed in Tables 1–4. For the time segments before the GRB trigger and after the GRB episode, the lightcurves are dominated by Poisson noise. Therefore the number of points obtained in the *pdf* for these time segments are small. This results in very poor fit statistics. The variation of the parameters of the Gaussian distributions with the evolution of the burst reflects the non-stationarity of the underlying random process. We also attempted to fit the *pdfs* with log-normal functions but the fitting with Gaussian function was found to be statistically better than the log-normal distribution. There is no definite correlation between the peak position and width of the Gaussians. It is very clear that the time-averaged probability density function profile (represented in *black*) can be fitted with multiple Gaussian functions. The possible physical interpretation of the Gaussian distribution is discussed below. It is argued that the Gaussian distribution possibly indicates the presence of turbulence in the GRB outflow originated in a relativistically expanding fireball. Possible consequences of the turbulence in the spectral evolution of each of the selected GRBs are also discussed in detail.

**Table 3. GRB061121:** Same as Table 1

Time (sec)	Gaussian Parameters				$\chi^2/\nu$
	$M$	$A_i$	$\mu_i$	$\sigma_i$	
−3 — 10 (red)	1	$408.1 \pm 14.4$	$0.07 \pm 0.01$	$0.14 \pm 0.01$	1.6/2
10 — 60 (green)	1	$2374 \pm 144$	$-0.01 \pm 0.01$	$0.1 \pm 0.004$	0.9/2
60 — 70 (blue)	2	$115.4 \pm 5.5$ $49.5 \pm 4.2$	$0.52 \pm 0.01$ $1.25 \pm 0.02$	$0.26 \pm 0.01$ $0.18 \pm 0.02$	10.3/12
70 — 80 (magenta)	4	$54.8 \pm 13.5$ $44.6 \pm 2.8$ $37.2 \pm 6.1$ $12.4 \pm 1.4$	$0.35 \pm 0.02$ $0.97 \pm 0.07$ $1.85 \pm 0.05$ $2.87 \pm 0.04$	$0.16 \pm 0.03$ $0.39 \pm 0.14$ $0.24 \pm 0.04$ $0.32 \pm 0.05$	12.5/22
80 — 95 (cyan)	1	$581.0 \pm 6.9$	$0.09 \pm 0.002$	$0.10 \pm 0.002$	0.3/2

**Table 4. GRB080411:** Same as Table 1

Time (sec)	Gaussian Parameters				$\chi^2/\nu$
	$M$	$A_i$	$\mu_i$	$\sigma_i$	
−10 — 0 (red)	1	$359.2 \pm 26.8$	$-0.02 \pm 0.02$	$0.14 \pm 0.01$	0.4/2
10 — 16 (green)	1	$293.9 \pm 18.7$	$0.43 \pm 0.02$	$0.20 \pm 0.01$	17.0/5
22 — 39 (magenta)	1	$396.4 \pm 19.1$	$0.08 \pm 0.02$	$0.21 \pm 0.01$	8.3/5
48 — 70 (yellow)	1	$442.3 \pm 23.5$	$0.27 \pm 0.01$	$0.20 \pm 0.01$	12.8/4

## 4.2 *pdf* and Turbulence

It is shown by Kumar & Narayan (2009) and Zou et al. (2009) that the optical and gamma-ray spectra in the prompt emission of GRB080319B can not be explained in the framework of internal shock model. Instead, Narayan & Kumar (2009) proposed the relativistic turbulence model to explain the prompt emission spectra of GRB080319B. In the framework of this model the highly variable gamma-ray lightcurve can be produced due to the emission from randomly moving eddies in the turbulence. The random relativistic variations of velocities of eddies cause the large amplitude variations in the individual pulses in gamma-ray burst lightcurve. In case of GRB080319B the optical emission is produced by synchrotron process in the inter-eddy medium whereas the gamma-rays are produced by inverse Compton process by energetic electrons in the eddies in the turbulence. To understand the probability density function obtained for the X-ray lightcurve of GRB080319B we argue as follows.

If the large amplitude variations are due to the random velocity fluctuations in turbulent eddies then the statistical properties of the velocity fluctuations are expected to be translated into the random fluctuations of the lightcurves. In recent works by Mouri et al. (2002) and Chu et al. (1996), it has been observationally shown that the probability density function of turbulent velocity fluctuations is Gaussian

for fully developed turbulence. The probability density function is sub-Gaussian when turbulence is developing and it is hyper-Gaussian during the decay of turbulence. We assume that these properties are also satisfied by the random velocity fluctuations in relativistic turbulence. In such a condition the intensity fluctuations in GRB lightcurve (which are supposed to be due to the velocity fluctuations of turbulent eddies) should also follow a Gaussian probability density function. In Figures 1–4 (*second panel*) the *pdfs* are shown for GRB080319b, GRB050525, GRB061121 and GRB080411 respectively. The *pdfs* for different time segments are shown in different colour and the time-averaged *pdf* is represented in *black*. The colour sequence is maintained same in all GRBs. It is to be noticed that the *pdfs* corresponding to the rising and falling edges of GRBs are completely separated from other *pdfs* corresponding to different time segments. In case of GRB080319b the *pdf* corresponding to a single segment is fitted with a single Gaussian function whereas for GRB050525 and GRB061121 *pdfs* corresponding to a single segment are fitted with multiple Gaussian functions. Multiple Gaussian distributions corresponding to a single lightcurve segment possibly indicate more than one region of turbulence in the GRB outflow. If we compare the rising and falling portions of GRBs with the development and decay of turbulence respectively then the corresponding peaks could be sub- and hyper-Gaussian distributions respectively. But such conclusion is very difficult to make with the present data.

At this point it is important to mention that in presence of intermittency, the turbulence statistics deviates from Gaussian behaviour (Falcon et al. (2010); Vassilicos (1995)). Generally when the amplitude of fluctuations are small, the turbulence statistics is Gaussian in case of fluid turbulence. In case of magnetohydrodynamic turbulence intermittency is generally present. The origin and nature of intermittency in fluid as well as magnetohydrodynamic turbulence is not known. Therefore any departure of the peaks in observed probability density functions from Gaussian distribution does not rule out the present interpretation of *pdf*. Particularly, if we consider the *pdf* of GRB080411 (Figure 4), we can see that the *pdfs* corresponding to the *red*, *green*, *magenta* and *yellow* portions of the lightcurve can be fitted with one or more Gaussian functions, but the *pdfs* corresponding to the peaks (*blue* and *cyan*) can not be fitted with Gaussian functions at all. It appears more like a power-law. Here we have not deliberately fitted them with any functional form. Having argued that the *pdfs* actually reflect the turbulence origin of GRB, now we concentrate on the spectral properties of GRB to see if those properties can be explained in terms of turbulence.

### 4.3 Turbulence, particle acceleration and spectral evolution of GRBs

#### 4.3.1 Turbulence and particle acceleration

The major challenge in high energy astrophysics is to understand the process of accelerating charged particles to relativistic energies so that they can emit high energy radiation in a given physical condition. It is generally assumed that the first order Fermi acceleration across a shock (internal or external) accelerates particles to relativistic energies with

a non-thermal distribution. But GRB models in general do not discuss this issue in detail. In presence of turbulence which is presumably magnetohydrodynamic in GRB outflow the particles can be accelerated by stochastic acceleration process or by magnetic reconnection process. In case of stochastic acceleration particles interact with the MHD waves developed in the plasma flow. This is a second order Fermi process and it is generally less efficient compared to the shock acceleration process. Lazarian et al. (2003) discussed that the stochastic acceleration process can be more efficient if momentum diffusion rate is higher than the pitch angle scattering rate and that is possible for a low density plasma in presence of high magnetic field. In such a condition the Alfvén speed (in the units of  $c$ ) exceeds unity and such conditions exist in GRB outflow (Lazarian et al. (2003)). Mao & Wang (2011) discussed jitter radiation in small scale random magnetic field generated by turbulence. Following Honda & Honda (2005), they considered that particles are accelerated in small scale random magnetic field. In such a condition, particle and photon spectra depend on the energy spectrum of turbulence.

Otherwise also particle acceleration in presence of turbulence is possible through magnetic reconnection which is obvious in MHD turbulence. Turbulence possibly accelerates the reconnection process. Lazarian & Vishniac (1999) first put forward the turbulence reconnection model and de Gouveia Dal Pino & Lazarian (2003) discussed the particle acceleration in turbulent reconnection. In general particles can be accelerated almost instantly by magnetic reconnection process, but this does not generate a power-law spectrum of particles. But de Gouveia Dal Pino & Lazarian (2003) and Lazarian et al. (2011) showed that the particle acceleration in turbulent reconnection is a first order Fermi process and a particle's energy changes after each crossing of the reconnection zone. The average fractional gain in energy is proportional to the reconnection speed. The magnetic flux from two neighbouring regions of the fluid approach each other with the reconnection speed. It was shown by de Gouveia Dal Pino & Lazarian (2003) that the resultant particle spectrum is a power-law with spectral index  $-2.5$ . This is steeper than the spectrum ( $\gamma^{-2}$ ) obtained with shock acceleration process,  $\gamma$  being the particle Lorentz factor. Larrabee et al. (2003) also studied the lepton acceleration by relativistic collisionless magnetic reconnection. They obtained a distribution function for electrons which varies as  $\sim \gamma^{-1}$ , but the final spectrum (what the authors called apparent spectrum) depends on the distribution function of the maximum Lorentz factor of electrons in each reconnection event. This makes the electron distribution  $\sim \gamma^{-1-q}$  where  $q > 1$ .

#### 4.3.2 Spectral properties

We study the following spectral properties of GRBs of our sample to understand if turbulence can explain the observed results.

- **Spectral evolution :** To study the spectral evolution of selected GRBs we extract the spectrum for every 5 sec for GRB080319b, GRB061121 and GRB080411 and for every 2.5 sec for GRB050525. For the first three GRBs, the photon spectra in the 15–150 keV energy range are fitted with

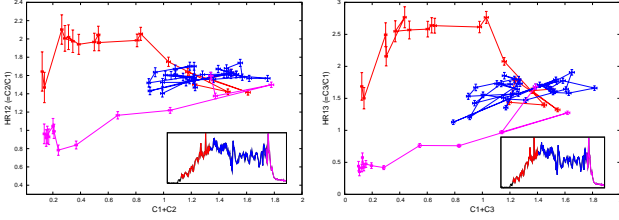


**Figure 5.** GRB080319B: *Left panel* : Hardness – count-rate diagram for energy bands  $E_1$  (15–25 keV) and  $E_2$  (25–50 keV), *Right panel* : Hardness – count-rate diagram for energy bands  $E_1$  (15–25 keV) and  $E_3$  (50–100 keV). The colours used for different portions of the lightcurves (plotted as inset in each panel) are in direct correspondence with the colours used in hardness – count-rate diagram.

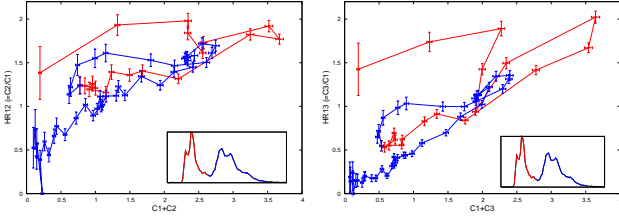


**Figure 6.** GRB050525: same as Figure 5.

power-law ( $\sim \epsilon^{-\alpha}$ ), whereas for the last one the spectra are fitted with a power-law with exponential cut-off. The spectra are fitted using  $\chi^2$  minimization process within XSPEC. For GRB080319b, GRB061121 and GRB080411, the magnitude of spectral index grossly increases as the burst evolves, indicating that the spectrum evolves from hard-to-soft with time. This is indeed observed for other bursts reported in the literature. The value of photon spectral index varies from  $\sim 0.6$  to  $\sim 2.1$  for GRB080319b, from  $\sim 1.3$  to  $\sim 1.8$  for GRB061121 and from  $\sim 1.1$  to  $\sim 2.6$  for GRB080411. It is to be noted that the evolution of spectral index is model dependent. Here the spectra are fitted with a single power-law which is statistically adequate due to the narrow energy bandwidth of the detector. It was shown by Band et al. (1993) that the GRB spectra, over a broader energy range are well-fitted with a smoothly broken spectrum (Band spectrum). The observed spectral index variation reflects the evolution of underlying GRB spectrum which is intrinsically a smoothly broken spectrum with different spectral slopes on two sides of the break energy. If we consider the turbulent reconnection responsible for the acceleration of particles to relativistic energies and synchrotron process is the basic radiation mechanism then the value of photon spectral index should be around 1.75 for instantaneous spectrum and 2.25 for cooling dominated spectrum. But the value of observed photon spectrum indices fall below these limits. This implies that even if turbulent reconnection plays an important role in accelerating particles in GRB outflow, it is not the only mechanism working there. This requires further detailed study.

In case of GRB050525, the spectral evolution pattern is not very clear because of its short duration. The spectra of this GRB could not be fitted well with power-law, instead a power-law with exponential cut-off fitted the spectra well.

• **Colour-colour diagram** : The hardness ratio between the two energy bands, say  $E_1$  and  $E_2$ , is defined as

$$HR_{12} = \frac{C_1}{C_2} \quad (3)$$

where  $C_1$  and  $C_2$  are the count rates in the energy bands  $E_1$  and  $E_2$  respectively. The error in the estimation of hardness ratio is

$$\Delta HR_{12} = \sqrt{\left(\frac{\Delta C_1}{C_1}\right)^2 + \left(\frac{\Delta C_2}{C_2}\right)^2} \quad (4)$$

Similarly the hardness ratio  $HR_{13}$  and its error  $\Delta HR_{13}$  can be defined for the energy bands  $E_1$  and  $E_3$ .

Colour-colour diagrams, shown in Figure 1–4 (*fourth panel*), show the correlations between the hardness  $HR_{12}$  and  $HR_{23}$ . These plots also have similar colour sequence as the lightcurves and are generated for the active part of the GRB lightcurves. The time resolutions used for these plots are 1 sec (GRB080319b, GRB080411) and 200 msec (GRB050525, GRB061121). It is generally found that the colour-colour diagrams show systematic correlations over the complete evolution of all bursts. The striking feature for the colour-colour diagrams for all GRBs is that they start with a very hard spectrum. This is possibly due to the almost instantaneous acceleration of particles to high energies. This could be possible in magnetic current filaments generated in turbulence. The estimated acceleration time scale for such event is given by Mao & Wang (2011). It depends on magnetic field strength and turbulent length scale in the flow. Later part of the evolution in colour-colour plane is primarily dominated by the cooling of particles. This makes the particle spectrum steeper and so the photon spectrum. It is important to note that in case of GRB080319b, the blue and magenta points (Figure 1, *fourth panel*) in colour-colour plane are clustered in a small region. These points correspond to the nearly flat portion of the lightcurve (represented in same colours). During this portion particle acceleration rate and cooling rate were comparable, thereby making the hardness almost constant.

• **Hardness–Count rate correlation** : The hardness and count rate correlations have been studied for the active phase of each GRB for the energy bands  $E_1$  (15–25keV),  $E_2$  (25–50keV) and  $E_3$  (50–100keV). For each burst, hardness vs countrate plots are shown in Figures 5 – 8. The left panel in each figure shows the hardness vs count rates calculated for energy bands  $E_1$  and  $E_2$  while the right panel shows the same for energy bands  $E_1$  and  $E_3$ . The representative colours in the lightcurve show the corresponding portions mapped into the hardness-count rate plane. The lightcurves used for this calculation had a time resolution of 200 ms except for GRB080319B where the lightcurves had time resolution of 1 sec. All hardness-count rate loops for GRB080319B, GRB080411 and GRB050525 are in clockwise sense except for the burst GRB061121. For GRB061121 the loop structure is quite complex. It starts with an anticlockwise loop for the first peak (*red portion*), then it traverses clockwise path for the second (*blue*) and it goes anticlockwise for the third peak (*pink*). The clockwise loops represent soft lag whereas the anticlockwise loops indicate hard lag (Kirk et al. (1998)). This is possibly due to the fact that during the fast rise of the spike, more particles are accelerated quickly to higher energies by some acceleration process.



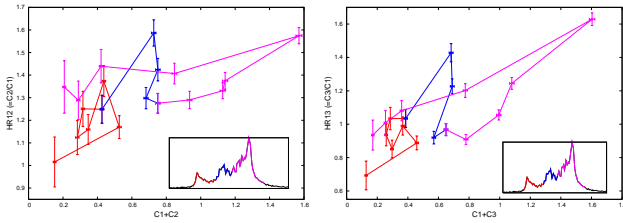


**Figure 7.** GRB061121: same as Figure 5.

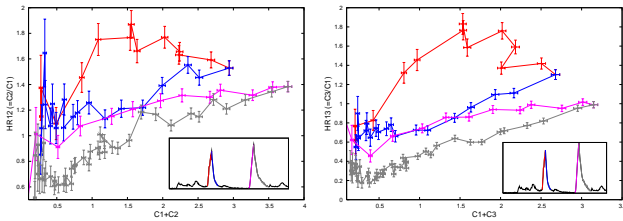


**Figure 8.** GRB080411: same as Figure 5.

During the decay part of the spike the cooling of the particles dominates and generates soft lag in the spectral evolution. This feature is very well reflected in the hardness–count rate loops shown in Figures 5 – 8. The clockwise loops arise when the evolution of spectral slope is primarily governed by any cooling process which is faster for higher energy particles (Kirk et al. (1998)). For GRB061121 anti-clockwise loops, signifying hard lag, appear when the acceleration time scale is nearly equal to the cooling time scale and particles are gradually accelerated to higher energies (Kirk et al. (1998)). These behaviours of spectral evolution of GRBs strongly depend on the particle acceleration process and the radiation emission mechanism occurring in the GRB outflow. With the present understanding of particle acceleration process in turbulence, it is not completely understood what kind of particle acceleration and cooling process can really explain such properties along with the evolution of the exact spectral forms.

## 5 CONCLUSION

In this paper we studied the time-dependent probability density function obtained from the observed lightcurves of four bright *Swift* gamma-ray bursts. The probability density functions are fitted with Gaussian distribution function. The parameters of the distribution function vary with time as the burst evolves. Considering the fact that the short time-scale flux variations in GRBs are due to the random motion of radiation emitting turbulent eddies, as proposed by Narayan & Kumar (2009), we argued that the Gaussian probability density function actually reflects the presence of turbulence in GRB outflow during the prompt emission.

We also studied the spectral properties of GRBs, such as the time evolution of spectral index, colour–colour diagram and hysteresis loops to understand if they can be explained in the framework of turbulence. With the present understanding of particle acceleration in turbulence, it is found that the particle acceleration process in turbulent reconnection can partially explain the observed spectral indices in 15–150

keV energy range. The behaviour reflected in colour–colour diagrams are consistent with spectral evolution seen for all GRBs. But deeper understanding of colour–colour diagrams and hysteresis loops require detailed knowledge of different time scales, therefore a detailed study of radiative processes in GRBs is essential and is beyond the scope of this paper. Finally, we would like to remark that for steady sources like X-ray binaries (*e.g.* Cyg X-1, (Wu et al. (2010); Uttley et al. (2005))) and flaring systems like solar flares (Zhang (2007)), the probability density functions are found to follow log-normal distributions. For both types of systems turbulence seems to a major role. In the light of such observations the main finding of this work, *i.e.* the Gaussian probability density functions for GRBs needs further study.

## 6 ACKNOWLEDGEMENT

Authors acknowledge Sudhir Jain for fruitful discussion on the probability density functions, Abhas Mitra for suggesting a relevant literature and the anonymous referee for very useful suggestions which enhanced the focus of the paper.

## REFERENCES

- Band D., Cummings J., Perri M., Holland S., Burrows D. N., Gehrels N., Hill J. E., Kennea J. A., Hunsberger S., Markwardt C., Palmer D., 2005, GRB Coordinates Network, 3466, 1
- Band D., Matteson J., Ford L., Schaefer B., Palmer D., Teegarden B., Cline T., Briggs M., Paciesas W., Pendleton G., Fishman G., Kouveliotou C., Meegan C., Wilson R., Lestrade P., 1993, *ApJ*, 413, 281
- Beloborodov A. M., Stern B. E., Svensson R., 2000, *ApJ*, 535, 158
- Bendat J. S., Piersol A. G., 2010, *Random Data: Analysis and Measurement Procedures* (Wiley Series in Probability and Statistics). Wiley
- Chu C. R., Parlange M. B., Katul G. G., Albertson J. D., 1996, *Water Resources Research*, 32, 1681
- de Gouveia Dal Pino E. M., Lazarian A., 2003, *ArXiv Astrophysics e-prints*
- Falcon E., Roux S. G., Laroche C., 2010, *Europhysics Letters*, 90, 34005
- Ghirlanda G., Celotti A., Ghisellini G., 2002, *A&A*, 393, 409
- Ghisellini G., 2010, in A. Comastri, L. Angelini, & M. Cappi ed., *American Institute of Physics Conference Series Vol. 1248 of American Institute of Physics Conference Series*, What is the radiative process of the prompt phase of Gamma Ray Bursts?. pp 45–48
- Goodman J., 1986, *ApJ Letters*, 308, L47
- Honda M., Honda Y. S., 2005, *ApJ*, 633, 733
- Kirk J. G., Rieger F. M., Mastichiadis A., 1998, *A&A*, 333, 452
- Kobayashi S., Piran T., Sari R., 1997, *ApJ*, 490, 92
- Kobayashi S., Piran T., Sari R., 1999, *ApJ*, 513, 669
- Kumar P., Narayan R., 2009, *MNRAS*, 395, 472
- Larrabee D. A., Lovelace R. V. E., Romanova M. M., 2003, *ApJ*, 586, 72



- Lazarian A., Kowal G., Vishniac E., de Gouveia Dal Pino E., 2011, *Planetary and Space Science*, 59, 537
- Lazarian A., Petrosian V., Yan H., Cho J., 2003, *ArXiv Astrophysics e-prints*
- Lazarian A., Vishniac E. T., 1999, *ApJ*, 517, 700
- Lazzati D., Begelman M. C., 2010, *ApJ*, 725, 1137
- Lloyd-Ronning N. M., Petrosian V., 2002, *ApJ*, 565, 182
- Lyutikov M., 2006, *New Journal of Physics*, 8, 119
- Lyutikov M., 2009, *ArXiv e-prints*
- Lyutikov M., Blandford R., 2003, *ArXiv Astrophysics e-prints*
- Mao J., Wang J., 2011, *ApJ*, 731, 26
- Markwardt C., Barthelmy S., Barbier L., Cummings J., Fenimore E., Gehrels N., Hullinger D., Krimm H., Palmer D., Parsons A., Sakamoto T., Sato G., Suzuki M., Tueller J., 2005, *GRB Coordinates Network*, 3467, 1
- Marshall F. E., Barthelmy S. D., Baumgartner W. H., Beardmore A. P., Burrows D. N., Gehrels N., Godet O., Holland S. T., Krimm H. A., Markwardt C. B., McLean K. M., Pagani C., Page K. L., Palmer D. M., Stamatikos M., Starling R. L. C., Ukwatta T. N., Vetere L., Ward P. A., 2008, *GRB Coordinates Network*, 7584, 1
- Medvedev M. V., 2006, *ApJ*, 637, 869
- Mészáros P., Ramirez-Ruiz E., Rees M. J., Zhang B., 2002, *ApJ*, 578, 812
- Meszaros P., Rees M. J., 1993, *ApJ*, 405, 278
- Mészáros P., Rees M. J., 2000, *ApJ*, 530, 292
- Mouri H., Takaoka M., Hori A., Kawashima Y., 2002, *Phys. Rev. E*, 65, 056304
- Narayan R., Kumar P., 2009, *MNRAS*, 394, L117
- Paczynski B., 1986, *ApJ Letters*, 308, L43
- Page K. L., Willingale R., Osborne J. P., Zhang B., Godet O., Marshall F. E., Melandri A., Norris J. P., O'Brien P. T., Pal'shin V., Rol E., Romano P., Starling R. L. C., Schady P., Yost S. A., Barthelmy S. D., Beardmore A. P., Cusumano G., Burrows D. N., De Pasquale M., Ehle M., Evans P. A., Gehrels N., Goad M. R., Golenetskii S., Guidorzi C., Mundell C., Page M. J., Ricker G., Sakamoto T., Schaefer B. E., Stamatikos M., Troja E., Ulanov M., Yuan F., Ziaeepour H., 2007, *ApJ*, 663, 1125
- Preece R. D., Briggs M. S., Mallozzi R. S., Pendleton G. N., Paciesas W. S., Band D. L., 2000, *ApJS*, 126, 19
- Racusin J. L., Karpov S. V., Sokolowski M., Granot J., Wu X. F., Pal'Shin V., Covino S., van der Horst A. J., Oates S. R., Schady P., Smith R. J., Cummings J., Starling R. L. C., Piotrowski L. W., Zhang B., Evans P. A., Holland S. T., Malek K., Page M. T., Vetere L., Margutti R., Guidorzi C., Kamble A. P., Curran P. A., Beardmore A., Kouveliotou C., Mankiewicz L., Melandri A., O'Brien P. T., Page K. L., Piran T., Tanvir N. R., Wrochna G., Aptekar R. L., Barthelmy S., Bartolini C., Beskin G. M., Bondar S., Bremer M., Campana S., Castro-Tirado A., Cucchiara A., Cwiok M., D'Avanzo P., D'Elia V., Della Valle M., de Ugarte Postigo A., Dominik W., Falcone A., Fiore F., Fox D. B., Frederiks D. D., Fruchter A. S., Fugazza D., Garrett M. A., Gehrels N., Golenetskii S., Gomboc A., Gorosabel J., Greco G., Guarnieri A., Immler S., Jelinek M., Kasprovicz G., La Parola V., Levan A. J., Mangano V., Mazets E. P., Molinari E., Moretti A., Nawrocki K., Oleynik P. P., Osborne J. P., Pagani C., Pandey S. B., Paragi Z., Perri M., Piccioni A., Ramirez-Ruiz E., Roming P. W. A., Steele I. A., Strom R. G., Testa V., Tosti G., Ulanov M. V., Wiersema K., Wijers R. A. M. J., Winters J. M., Zarnecki A. F., Zerbi F., Mészáros P., Chincarini G., Burrows D. N., 2008, *Nature*, 455, 183
- Rees M. J., Meszaros P., 1992, *MNRAS*, 258, 41P
- Rees M. J., Meszaros P., 1994, *ApJ Letters*, 430, L93
- Sari R., Piran T., 1995, *ApJ Letters*, 455, L143+
- Sari R., Piran T., 1997, *ApJ*, 485, 270
- Shemi A., Piran T., 1990, *ApJ Letters*, 365, L55
- Tavani M., 1996a, *ApJ*, 466, 768
- Tavani M., 1996b, *Physical Review Letters*, 76, 3478
- Uttley P., McHardy I. M., Vaughan S., 2005, *MNRAS*, 359, 345
- Vassilicos J. C., 1995, *Nature*, 374, 408
- Wu Y. X., Belloni T. M., Stella L., 2010, *MNRAS*, 408, 2413
- Zhang S. N., 2007, *Highlights of Astronomy*, 14, 41
- Zou Y., Fan Y., Piran T., 2009, *MNRAS*, 396, 1163